

Wilforol A inhibits human glioma cell proliferation and deactivates the PI3K/AKT signaling pathway

Zhihan Wang, Li Ren, Hao Xu, Zilong Wei and Hongjun Zeng✉

Department of Neurosurgery, Pudong Hospital Affiliated to Fudan University, Shanghai, China

Objectives: To study the anti-proliferation activity of wilforol A against glioma cells and its possible molecular mechanisms. **Methods:** Human glioma cell lines U118 MG and A172, human tracheal epithelial cells (TECs) and astrocytes (HAs) were exposed to various concentrations of wilforol A and evaluated for viability, apoptosis, and levels of proteins using WST-8 assay, flow cytometry and Western blot analysis, respectively. **Results:** Wilforol A inhibited the growth of U118 MG and A172 cells, but not TECs and HAs, in a concentration-dependent manner and the estimated IC_{50} were 6 to 11 μ M after 4 h-exposure. Apoptosis was induced at an apoptotic rate of about 40% at 100 μ M in U118 MG and A172 cells, but the rates were less than 3% in TECs and HAs. Co-exposure to caspase inhibitor Z-VAD-fmk significantly reduced wilforol A-induced apoptosis. Wilforol A treatment also reduced the colony formation ability of U118 MG cells and triggered a significant increase in ROS production. Elevated levels of pro-apoptotic proteins p53, Bax and cleaved caspase 3 and reduced level of the anti-apoptotic protein Bcl-2 were observed in glioma cells exposed to wilforol A. The expression of PI3K and p-Akt genes in the PI3K/AKT pathways were significantly downregulated in glioma cells treated with wilforol A. **Conclusions:** Wilforol A inhibits the growth of glioma cells, reduces the levels of proteins in the P13K/Akt signal transduction pathways and increases the levels of pro-apoptotic proteins.

Keywords: glioma; natural product; anticancer activity; apoptosis, P13K/Akt signaling pathways

Received: 16 April, 2022; revised: 19 October, 2022; accepted: 09 January, 2023; available on-line: 16 February, 2023

✉e-mail: hongjunzeng723@yeah.net

Abbreviations: ANOVA, analysis of variance; DCFHDA, 2',7'-Dichlorofluorescein diacetate; EMEM, Eagle's minimum essential medium; EMT, epithelial-mesenchymal transition; FBS, fetal bovine serum; HAs, astrocytes; HRP, horseradish peroxidase; NR4A1, nuclear receptor subfamily 4 group A member 1; PI, propidium iodide; PVDF, polyvinylidene difluoride; RIPA, radioimmunoprecipitation assay buffer; ROS, reactive oxygen species; SEM, standard error of the mean; TECs, human tracheal epithelial cells

INTRODUCTION

Gliomas are the most common tumors with extremely broad range of clinical behaviors in the central nerve systems of children and adolescents, although the definitive cell of origin of gliomas still remains elusive (Cahill & Turcan, 2018; Sturm *et al.*, 2017). Gliomas are characterized based on histologic and molecular data into several entities including diffuse gliomas (astrocytoma, oligodendroglioma and glioblastoma) and low-grade gliomas (angiocentric glioma, pilocytic astrocytoma and sub-

ependymal giant cell astrocytoma). Genomic profiling of certain gliomas is necessary to define the histologic subtyping and proper use of prognostic and predictive biomarkers for treatment (Ferris *et al.*, 2017; Reifenberger *et al.*, 2017). Early and rational use of drugs that effectively inhibit the proliferation of glioma cells is important to obtain a good prognosis for patients (Morshed *et al.*, 2019). However, a significant portion of gliomas develop over a short period of time and progress rapidly into WHO grade III or IV high-grade gliomas. Despite all therapeutic efforts, gliomas remain largely incurable. Current treatment of gliomas relies on surgery in combination with chemotherapy and/or radiotherapy. However, many tumors show a high resistance to these interventions, and recurrences are very frequent since conventional therapies do not take into full account the unique molecular features of different subtypes of gliomas (Ghotme *et al.*, 2017). Several new therapies have been proposed to better manage the cancer, including immunotherapy that is able to penetrate the blood-brain barrier to deliver drugs to lymphatics with some promising results (Hanaei *et al.*, 2018; Xu *et al.*, 2020), use of IL15R α -IL15-armed oncolytic poxviruses in combination with adoptive T-cell therapy, rapamycin, and celecoxib (Xu *et al.*, 2020). In addition, several new strategies have been explored to treat glioma. For example, gene therapy based on lipid nanoparticles as non-viral vectors has been attempted to deliver genes across the blood-brain barrier to reach the glioma cell target (Luiz *et al.*, 2021) and ketogenic diets are suggested to induce ketosis to target the glycolytic phenotype to halt the progression of lower grade tumors to more aggressive subtypes (Poff *et al.*, 2019).

In the past decades, there have been growing interest in exploring natural medicinal plants and their bioactive molecules for potential anti-tumor activity, both *in vitro* and *in vivo* (Li *et al.*, 2019; Weng & Goel, 2022). Tripterine, also known as celastrol, is an active ingredient isolated from a vine plant *Tripterygium wilfordii*. It has been proven to have therapeutic effect on inflammatory response and tumors, including hepatoma, multiple myeloma, breast cancer, cervical cancer, prostate cancer and leukemia (Chen *et al.*, 2018b; Li *et al.*, 2021; Yang *et al.*, 2021). Using network pharmacology-based strategy, several components from *T. wilfordii* have been found to impact a number of signaling pathways, such as the Toll-like receptor signaling pathway, NF-kappa B signaling pathway and HIF-1 signaling pathway in acute myeloid leukemia (Fang *et al.*, 2020). Tripterine suppresses the malignancy of breast cancer by upregulating miR-184 (Wang, 2021) and inhibits cell proliferation by increasing the level of Bax in pancreatic cancer cells (Chen *et al.*, 2022). Studies also show that tripterine promotes autophagy and apoptosis *via* the ROS/JNK and AKT/

mTOR signaling pathways in glioma cell lines U251, U87-MG and C6 (Liu *et al.*, 2019) and blocks the PI3K/AKT/mTOR signaling pathway to suppress vasculogenic mimicry formation and angiogenesis (Zhu *et al.*, 2020). On the other hand, wilforol A, a triterpenoid and analog of celastrol from the same plant, has not been characterized for its anticancer activity.

The purpose of this study was to investigate the effect of wilforol A on proliferation of cancer cells and its possible molecular mechanisms underlying the anticancer activity using glioma cell lines U118 and A172.

MATERIALS AND METHODS

Cell lines

Two human glioma cell lines U118 MG, A172, and human tracheal epithelial cells (PCS-300-013, TECs) were purchased from American Type Collection Center (ATCC), USA, and cultured in Eagle's minimum essential medium (EMEM) containing 10% fetal bovine serum (FBS) at 37°C in 5% CO₂. Cells were digested with 0.25% trypsin for 3 min when reaching 80–90% confluence, pelleted by centrifugation at 25°C and subcultured in fresh EMEM medium with 10% FBS under the same culture conditions. Human astrocytes (HAs) were purchased from iXCells (San Diego, CA, USA) and grown in astrocyte medium (cat no. 10HU-035, iXCells) at 37°C in 5% CO₂. Adenovirus with and without the Akt gene (AD00306Z) were purchased from Creative Biogene, USA, and used to infect cells at 1×10¹⁰ PFU/ml according to the supplier's protocols to generate Akt-overexpressing cells.

Cell viability assay

The viability of cells was measured using Cell Counting Kit 8 (WST-8, Abcam, USA) based on the supplier's instructions. Wilforol A purchased from TargetMol, MA, USA, was dissolved in 1% DMSO (molecular biology grade, Sigma, USA) as stock solution. Cells were seeded in the wells of 24-well black culture plates at the density of 1×10⁴ per well in 100 µl EMEM medium and cultured at 37°C in a 5% CO₂ incubator. After incubation for 24 h, 100 µl EMEM medium containing various concentrations of wilforol A and 0.2% DMSO was added to each well and cells were cultured at 37°C in a 5% CO₂ incubator for another 4 h. EMEM medium containing 0.2% DMSO was used as control. Cells were then added with 20 µl WST-8 solution and incubated in the dark at 37°C for 2 h. The absorbance at 450 nm was measured using a plate reader. The experiments were independently repeated three times and all samples were tested in triplicate.

Soft agar assay

Soft agar assays were performed to assess the colony formation ability as described previously (Horibata *et al.*, 2015). Briefly, U118MG cells (5×10⁶ cells/ml) were suspended gently in 0.6% type VII agarose that was maintained at 42°C and prepared in EMEM medium supplemented with 10% FBS and 1% penicillin/streptomycin. The cells were poured to the bottom of 60-mm dishes to form a bottom layer over 1.2% agar. After being solidified at 25°C for 30 min, the plates were sealed and were placed into a humidified incubator for culture at 37°C. Two weeks later, the colonies were stained overnight with 200 µl of 0.1% crystal violet per

well at 37°C. The stained colonies were analyzed using a colony counter.

Flow cytometry

After exposure to wilforol A for 4 h, cells (5×10⁶) were pelleted by centrifugation at 1000 rpm at 25°C for 10 min and resuspended in 500 µl PBS. For assessment of apoptosis, the cells were washed twice with 500 µl PBS, added with 10 µl Annexin V and propidium iodide (PI) from Annexin V-DY-634 PI Apoptosis Staining/Detection Kit (Abcam) to stain the cells according to the manufacturer's instructions. For assessment of autophagy, cells were stained with autophagy probes in Autophagy Assay Red Detection Kit (cat. no. APO010B, Biorad, USA) according to the manufacturer's instructions. For determination of necrotic cells, GFP-CERTIFIED Necrosis detection kit (cat. no. ENZ5100225, Enzo Life Sciences, Thermo Fisher, USA) was used to detect necrotic cells with the FL 3 channel as instructed by the manufacturer. The stained cells were loaded and analyzed on a NovoCyte flow cytometer (Agilent, USA). The quantitation of cells was calculated by the built-in CellQuest software. To assess the effect of caspase inhibitor, 50 µM of Z-VAD-fmk (Alexis Biochemicals, San Diego, CA) was added to the culture medium. For reactive oxygen species (ROS) analysis, cells were exposed to wilforol A for 4 h and stained with DCFH-DA (cat. no. S0033S, Beyotime, Beijing, China) in serum-free medium (after 1:1000 dilution) at the final concentration of 10 µmol/L. After incubation at 37°C for 20 min, cells were washed three times with serum-free medium to remove recessive DCFH-DA and loaded to the cytometer for analysis according to the supplier's protocols. The experiments were independently repeated three times and all samples were tested in triplicate.

Western blot

After exposure to wilforol A for 4 h, cells (5×10⁶) were pelleted by centrifugation at 1000 rpm at 25°C for 10 min and were lysed in RIPA buffer (Thermo Fisher Scientific, USA) that contains protease inhibitors cocktail to minimize protein degradation. Proteins in the lysates were quantitated using BCA kit (Thermo Fisher Scientific) according to manufacturer's instructions. After denaturing by boiling at 100°C for 5 min, the proteins were loaded onto 12% polyacrylamide gels, separated by electrophoresis and transferred to PVDF membranes (Millipore, USA). The proteins of interest were detected by incubating with primary antibodies against p53 (cat. no. AF7671), Bax (cat. no. AF1270), Bcl-2 (cat. no. AF0060), cleaved caspase 3 (cat. no. AF1213), PI3K (cat. no. AF1549, specific for subunit p110 α), Akt (cat. no. AF0045), p-Akt (Ser473) (cat. no. AA329), p-Akt (Thr308) (cat. no. AA331) and β -actin (cat. no. AF5001) (all from Beyotime) and secondary antibody (goat anti-human IgG H&L (HRP) (cat. no. ab97161, Abcam). The immunoreactive bands were captured using Chemi Doc XRS plus chemiluminescence imaging system (Bio-Rad, USA) after visualization with a chemiluminescence kit (Thermo Fisher Scientific). The gray values of the bands on the blots were determined using Quantity One software.

Statistical analysis

All data were shown as means \pm standard error of the mean (SEM) obtained from three independent experiments. Statistical comparisons among groups were

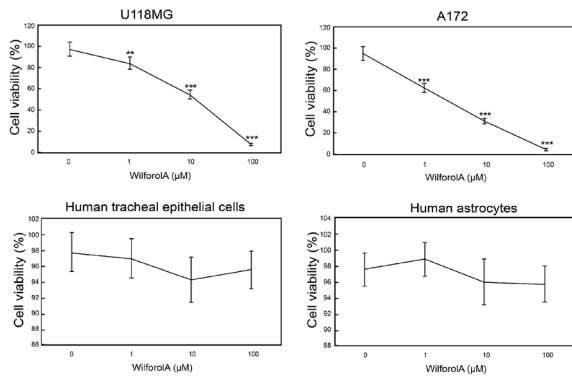


Figure 1. Viability of U118MG cells, A172 cells, tracheal epithelial cells and human astrocytes after exposure to Wilforol A for 4 h.

The viability was measured with the cell Counting Kit 8 (WST-8). 1×10^4 cells/well were seeded cultured overnight in a black wall 24-well plate. Cells were treated with diluted Wilforol A for 4 hours. The absorbance was measured at 460 nm using a plate reader. The experiments were independently repeated three times. One-way ANOVA was used to analyze the differences. ** and *** denote <0.01 , and 0.001 , respectively, compared to control.

assessed using one-way analysis of variance (ANOVA). A value of $P < 0.05$ was considered statistically significant.

RESULTS

Wilforol A reduces the viability of glioma cells

We first tested the effect of wilforol A on the viability of glioma cell lines U118 MG and A172 using WST-8 assays. After 4 h exposure to wilforol A, the viability of cells in both cell lines began to decline at $1 \mu\text{M}$ wilforol A and decreased from over 95% in controls to 8% in U118MG and 5% in A172 at $100 \mu\text{M}$ wilforol A, indicating that wilforol A is potently toxic to glioma cells and the viability reduction is concentration-dependent (Fig. 1). The IC_{50} for U118 MG and A172 were estimated to be 11 and $6 \mu\text{M}$, respectively, suggesting that A172 is more sensitive to wilforol A. Furthermore, we tested if non-glioma cells could be inhibited by wilforol A within the concentration range using TECs and HAs. No inhibition was observed up to $100 \mu\text{M}$ wilforol A (Fig. 1), suggesting that wilforol A is more toxic to glioma cells.

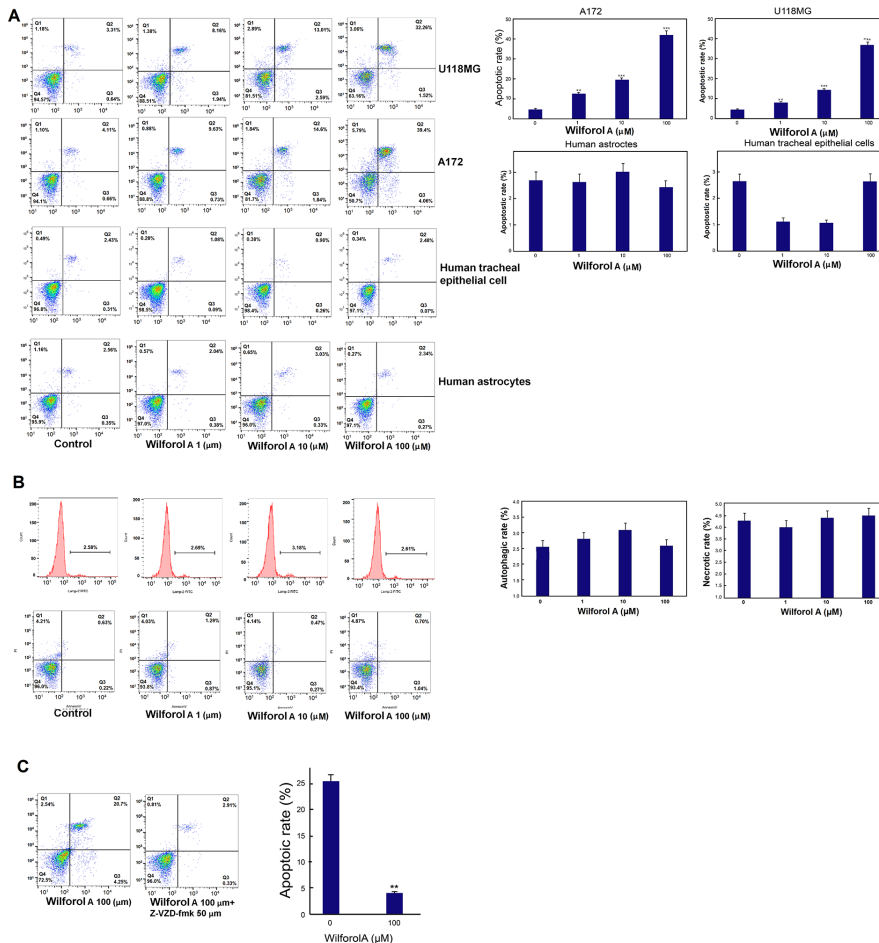


Figure 2. Apoptosis (A), autophagy and necrosis (B) of U118MG and A172 cells after exposure to wilforol A (A) and Z-VAD-fmk (C) for 4 h.

The apoptosis, autophagy and necrosis were measured with Annexin V- DY-634 PI Apoptosis Staining / Detection Kit, Autophagy Assay Red Detection Kit and GFP-CERTIFIED Necrosis detection kit. Cells (5×10^6) were seeded overnight in a black wall 24-well plate and were treated with diluted Wilforol A and $50 \mu\text{M}$ Z-VAD-fmk for 4 hours. The treated cells were stained with relevant probes and analyzed on NovoCyte flow cytometer. Left panel: representative flow cytometry results; right panel: statistical results of apoptosis. The experiments were independently repeated three times. One-way ANOVA was used to analyze the differences. ** and *** denote <0.01 , and 0.001 , respectively, compared to control.

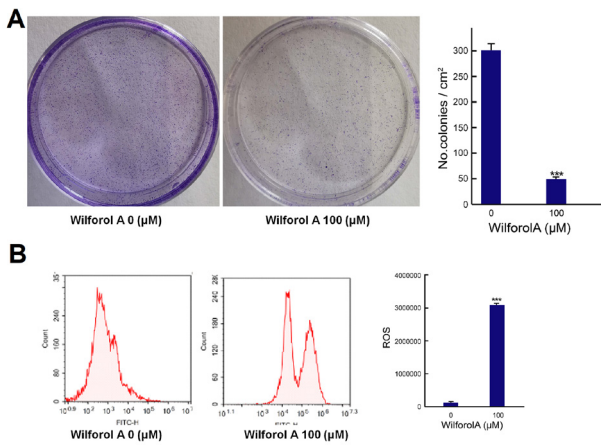


Figure 3. Colony formation and ROS production of U118MG after exposure to wilforol A for 4 h. U118MG cells were suspended 0.6% agarose prepared in EMEM medium. The cells were poured to the bottom of 60-mm dishes and cultured at 37°C for weeks. The colonies were stained with 0.1% crystal violet and analyzed. (A) left panel: colony formation in soft-agar, right panel: number of colonies. (B) U118MG cells (5x10⁵cells/ml) were incubated with 100 μM wilforol A for 4 h and reacted with DCFH-DA in serum-free medium. After incubated at 37°C for 20 m, cells were loaded to the cytometer for analysis according to supplier's protocols. A, left panel: flow cytometry results, right panel: fluorescence density. The experiments were independently repeated three times. One-way ANOVA was used to analyze the differences. *** denotes <0.001, compared to control.

Wilforol A increases apoptosis, but not autophagy and necrosis in glioma cells

Apoptosis is one of the most important mechanisms leading to cell death after exposure to various cytotoxic agents. We therefore analyzed the apoptosis of U118MG and A172 cells after 4 h exposure to wilforol A at different concentrations using flow cytometry. Cells with both early and later apoptosis were detected after exposure to wilforol A, although the majority was later apoptosis at all of the tested concentration levels (Fig. 2A). After exposure to 100 μM wilforol A, over 95% of apoptotic cells were later apoptotic (Fig. 2A). Analysis showed that

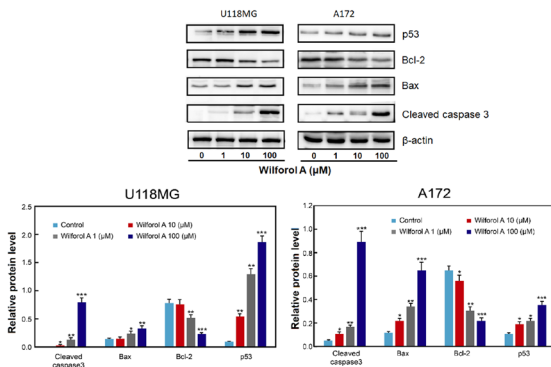


Figure 4. Expression of apoptosis-related proteins in U118MG and A172 cells after exposure to Wilforol A for 4 h. U118MG and A172 (5x10⁵) were seeded overnight in a black wall 24-well plate. Cells were treated with diluted Wilforol A for 4 hours. The treated cells were harvested, and total proteins were extract using RIPA buffer and separated on 12% SDS-PAGE. Proteins of interest were detected with relevant antibodies and visualized with a chemiluminescence kit. Upper panel: representative Western blots; lower panel: statistical results of protein expressions. The experiments were independently repeated three times. One-way ANOVA was used to analyze the differences. * ** and *** denote <0.05, 0.01, and 0.001, respectively, compared to control.

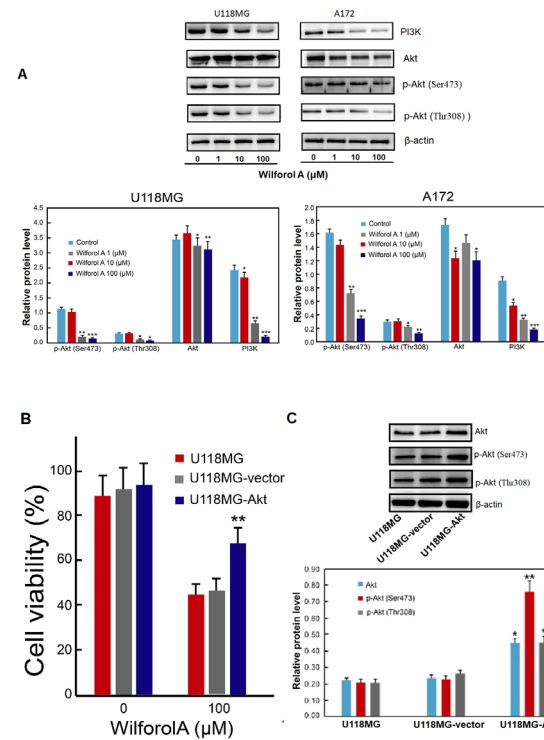


Figure 5. Levels of the PI3K/AKT signaling pathway proteins (A) in U118MG and A172 cells, viability of Akt-overexpressing U118MG cells (B) and levels of the Akt (C) after exposure to Wilforol A for 4 h. U118MG and A172 (5x10⁵), or U118MG infected with Akt over-expression vector were seeded overnight in a black wall 24-well plate. Cells were treated with diluted Wilforol A for 4 hours. The treated cells were harvested, and total proteins were extract using RIPA buffer and separated on 12% SDS-PAGE. Proteins of interest were detected with relevant antibodies and visualized with a chemiluminescence kit. The viability was measured with the cell Counting Kit 8 (WST-8). 1x10⁴ cells/well were seeded cultured overnight in a black wall 24-well plate. Cells were treated with diluted Wilforol A for 4 hours. The absorbance was measured at 460 nm using a plate reader. A, Upper panel: representative Western blots; lower panel: statistical results of protein contents. B, results of viability assays; C, Upper panel: representative Western blots; lower panel: statistical results of protein levels. The experiments were independently repeated three times. One-way ANOVA was used to analyze the differences. * ** and *** denote <0.05, 0.01, and 0.001, respectively, compared to control.

in both cell lines the total apoptotic rates increased from less than 5% to around 40% as the concentration of wilforol A increased from 1 μM to 100 μM (Fig. 2A). Similar to viability reduction, A172 cells had slightly more apoptotic cells than U118MG cells at the same wilforol A concentrations (Fig. 2A). On the other hand, no increase in apoptosis was observed in TECs and HAs after exposure to up to 100 μM wilforol A as compared to the controls (Fig. 2A). Autophagy and necrosis are also important pathways leading to cell death, and were assessed in U118 MG after exposure to wilforol A. The data showed that there was no significant change in autophagic and necrotic cells as compared to the unexposed cells (Fig. 2B).

To further confirm that apoptosis pathway is involved in the observed viability reduction, U118MG cells were treated with caspase inhibitor Z-VAD-fmk. The results showed that this treatment partially reduced wilforol A-induced apoptosis, suggesting that caspase is likely involved in the induced apoptosis (Fig. 2C).

Wilforol A reduces colony formation ability and triggers ROS production in glioma cells

To further assess the cytotoxicity of wilforol A to glioma cells, the colony formation ability of U118MG was assessed using soft-agar assays. The results showed that after treatment with wilforol A, the colony formation ability of U118MG was significantly reduced (Fig. 3A) and ROS production was significantly increased (Fig. 3B).

Effect of wilforol A on the level of apoptosis-related proteins

Western blot analyses showed the levels of apoptosis-related proteins p53, Bax and cleaved caspase 3 were increased, while Bcl-2 level was reduced in both cell lines after exposure to wilforol A (Fig. 4). Statistical analysis showed that the changes in the levels of these proteins were wilforol A-concentration-dependent and the greatest changes in the levels occurred at the highest wilforol A concentration (Fig. 4). While the changes in the protein levels in the two cell lines showed similar trends in response to wilforol A exposure, there were more increases in the levels of cleaved caspase 3 and higher p53 level in U118MG than in A172 cells, while Bax increased more in A172 than in U118MG cells (Fig. 4).

Effect of wilforol A on levels of PI3K/Akt signaling pathway proteins

PI3K/AKT signaling pathway plays a very important role in cancer and the epithelial-mesenchymal transition (EMT) (Xu *et al.*, 2015). Western blot analyses showed that the production of PI3K/Akt signaling pathway protein PI3K, Akt and p-Akt (both p-Akt (Ser473) and p-Akt (Thr308)) was all downregulated after U118MG and A172 cells exposure to wilforol A and the decreases were concentration-dependent, although the downregulation of Akt was not as large as other proteins and was not concentration-dependent in A172 cells (Fig. 5). To consider the contribution of Akt in wilforol A-induced cell death, U118 MG overexpressing Akt was assessed for its sensitivity to wilforol A. Compared with U118 MG and U118 MG infected with an empty vector, U118 MG overexpressing Akt had significantly higher level Akt and p-Akt (both p-Akt (Ser473) and p-Akt (Thr308)) and higher viability, suggesting the Akt pathway is at least partially involved in the wilforol A-induced cell death (Fig. 5B and C).

DISCUSSION

Wilforol A is a pentacyclic triterpenoid with the formula C₂₉H₃₈O₅ and is one of the main active ingredients extracted from the medicinal plant *T. wilfordii*. Our experimental data indicated that wilforol A is potently and preferentially toxic to glioma cells with a IC₅₀ between 6 and 11 μM in U118MG and A172. It generates apoptosis, ROS; upregulates the production of apoptosis-related proteins and downregulates the levels of PI3K/AKT signaling pathway proteins, suggesting that more studies are warranted to investigate the anticancer activity of this compound and to explore its potential as candidate drug for cancer therapy.

Several molecules have been isolated from *T. wilfordii* that processes anticancer activity. For example, celastrol and triptolide are terpenes purified from *T. wilfordii* and have been demonstrated to be inhibitory to various cancer cells, such as promyelocytic leukemia, T cell lympho-

ma and hepatocellular carcinoma cell (Chan *et al.*, 2001; Meng *et al.*, 2011), cervical cancer cell (Kim *et al.*, 2010) and head and neck cancer cells (Cai *et al.*, 2021). However, wilforol A, which is an analog of these terpenes with structural similarity to celastrol, has not been sufficiently characterized for its activity against cancer, although it is recorded to have inhibitory activity against MIA-PaCa2 cells (hypotriploid human pancreatic cancer cells, IC₅₀=3 μM) and A549 cells (adenocarcinomic human alveolar basal epithelial cells, IC₅₀=3 μM) after 72 h exposure (<https://pubchem.ncbi.nlm.nih.gov/compound/Wilforol-A#section=Biological-Test-Results>). Our experimental data showed that wilforol A has a IC₅₀ of 6 to 11 μM for glioma cell lines A172 and U118 MG after 4 h exposure, but is not inhibitory to TECs and HAs, suggesting that there are differences in the toxicity of the compound to cell lines. It is also likely that the IC₅₀ would change over the exposure time, with longer exposure generating smaller IC₅₀. Previously, it was reported that the IC₅₀ of triptolide and celastrol are 0.21 and 2.58 μM for glioma cell line SHG44 after 48 h exposure (Zhou *et al.*, 2002). The difference in the response of cell lines to wilforol A might be attributed to their different cellular and molecular characteristics, such as cell membrane permeability and metabolic activity, because these cells were derived from different patients. After exposure to wilforol A, the colony formation ability of U118 MG was significantly reduced. Triptolide also inhibits the colony formation of breast cell lines MCF-7 and BT-20, stomach cancer cell lines MKN-45, MKN-7, and KATO-III, and promyelocytic leukemia cell line HL-60 (Wei & Adachi, 1991), implying that wilforol A may have anticancer activity against a broad range of cancers due to its structure similarity to celastrol and triptolide.

Several mechanisms have been proposed with regard to the inhibitory effect of these *T. wilfordii* compounds. For example, celastrol and triptolide may inhibit leukemia cell proliferation by inducing apoptosis and downregulating NF-κB activity and miR-16-1 (Chan *et al.*, 2001; Meng *et al.*, 2011). In cervical cancer cells caspase-dependent, mitochondria-mediated apoptosis results in loss of cell viability (Kim *et al.*, 2010) and in head and neck cancer gasdermin E-mediated pyroptosis is induced after suppressing mitochondrial hexokinase-II (Cai *et al.*, 2021). They not only directly induce apoptosis in cancer cells but also enhance apoptosis induced by tumor necrosis factor and downregulate the expression of inhibitors of apoptosis proteins (IAPs), such as IAP1 and IAP2 (Lee *et al.*, 1999). Similarly, apoptosis was observed in our experiments in both cell lines after the cells were exposed to wilforol A and increased as wilforol A concentration increases. Furthermore, exposure to caspase inhibitor Z-VAD-fmk reduced apoptosis induced by wilforol A as previously reported (Arita *et al.*, 2000; Yang *et al.*, 2003), indicating that apoptosis is likely one of the pathways leading to the inhibition of cell proliferation. Analysis showed that the pro-apoptotic proteins such as p53, Bax and cleaved caspase 3 were upregulated while the anti-apoptotic protein Bcl-2 was downregulated after wilforol A treatment. Also, these regulations are concentration-dependent and have similar trends in both cell lines, suggesting that similar apoptosis mechanisms are motivated after wilforol A treatment. Apoptosis is a very complex process in which the activation of caspase family genes plays an important role (Christgen *et al.*, 2020). Caspase 9 is a key protease in the endogenous apoptotic pathway at the top of caspase-cascade system that leads to the activation of caspase 3 to generate cleaved caspase 3, apoptosis and cell death (Nagata, 2018). How-

ever, since the apoptotic cells at the highest wilforol A concentration is about 40%, which is much less than the percentages of inviable cells determined by WST-8 assays, which were over 90%. The difference in cell death rate could be attributed to other causes of cell death, such as necrosis, pyroptosis and autophagy. In mice, celastrol acts as a nuclear receptor subfamily 4 group A member 1 (NR4A1) agonist and may induce autophagy in a Nur77-dependent manner (Hu *et al.*, 2017). However, our assessment showed that both autophagic and necrotic cells were not changed after exposure to wilforol A, suggesting that there might be other pathways of cell death that are involved in the wilforol A-induced cell injury, which needs to be identified to better understand the mechanisms underlying the anticancer activity of wilforol A (D'Arcy, 2019).

To further elucidate the mechanisms underlying the anticancer activity, we profiled the expression of proteins in the PI3K/AKT pathway, which is one of the most important signaling pathways that are crucial to many aspects of cell growth and survival (Porta *et al.*, 2014) and is often activated in various human cancers (Aoki & Fujishita, 2017), including gliomas (Li *et al.*, 2016). Akt may be activated to p-Akt by PI3K to promote or suppress a number of downstream molecules such as Bad, caspases, NF- κ B, mTOR and eNOS to play a leading role in regulating tumor development (Xia & Xu, 2015). In addition, Akt can also activate nuclear transcriptional factors NF- κ B to promote the expression of anti-apoptosis genes, such as c-Yaps and Bcl-2 that improve the survival and suppress apoptosis of tumor cells (Feng *et al.*, 2018). Furthermore, potentiated Akt and p-Akt have protective effect against cardiomyopathy (Zeng *et al.*, 2017). Our results showed that PI3K, Akt and p-Akt (phosphorylated at Ser473 or Thr308) are all downregulated in a concentration-dependent manner after the two cell lines were treated with wilforol A, although the downregulation of Akt is lower as compared to the other proteins and is not strictly concentration-dependent in A172 cells, suggesting that wilforol A might impact apoptosis in glioma cells through the PI3K/AKT signaling pathway. The reduction of total Akt might be attributed to reduced cell viability, which leads to lower metabolic activity. Furthermore, U118 MG overexpressing Akt1 was found less sensitive to wilforol A. This is consistent with previous finding that Akt overexpression decreases the chemosensitivity of gastric cancer cells to cisplatin (Zhang *et al.*, 2013), confirming that PI3K/AKT pathway is likely involved in wilforol A-induced cell death. However, a number of pathways and mechanisms might be involved in the control of viability. For instance, silencing FAM19A5 in the FAM19A5/S1PR1 signaling pathway significantly reduces the viability of mantle cell lymphoma (Wang, 2021), indirubin suppresses the viability of ovarian cancer cell through the STAT3 signaling pathway (Chen *et al.*, 2018a) and rhein induces cell death in hepaRG cells through the upregulation of proteins in the apoptotic pathways (You *et al.*, 2018). It is therefore essential to profile more signaling pathways to gain comprehensive understanding of wilforol A-induced cell death.

Although our data show that wilforol A suppresses the growth of glioma cells and induces apoptosis, it is unclear whether wilforol A exerts its biological activity from outside or inside of the cells, and if from inside of the cells, how the molecule enters the cells. Exposure of glioma cells to wilforol A generated increased ROS production, suggesting that it is likely that wilforol A exerts its biological activity from inside of the cells, because

mitochondria are major sites for ROS synthesis (Lucia *et al.*, 1997). However, more studies investigating cell membrane integrity, membrane potential changes and permeability are needed to understand the site of action of wilforol A. NR4A1 is mentioned as a target for wilforol A (<https://pubchem.ncbi.nlm.nih.gov/compound/Wilforol-A#section=Biological-Test-Results>). However, it is unclear whether the binding of wilforol A to NR4A1 results in the inhibition of cell growth. Previously, ectopic expression of NR4A1 was shown to enhance tumorigenesis by breast cancer cells (Guo *et al.*, 2021) and it may be possible that the binding of wilforol A to NR4A1 may deactivate NR4A1, resulting in reduced tumorigenesis. Furthermore, *T. wilfordii* is known to cause various adverse effects leading to leukopenia, gastrointestinal reactions, menstrual disorders and liver dysfunction when administered as crude extracts (Zhang *et al.*, 2016). However, whether purified wilforol A has adverse effects is largely unknown, and more studies are needed to further define the safety profiles and efficacy of this compound in *in vitro* and *in vivo* models.

Taken together, our experimental data have demonstrated that wilforol A has antiproliferative activity against glioma cells. It deactivates the PI3K/Akt signal transduction pathways, leading to reduced p-Akt expression and upregulated expression of pro-apoptosis genes, which might be responsible for increased apoptosis, and subsequently reduced proliferation of glioma cells.

REFERENCES

- Aoki M, Fujishita T (2017) Oncogenic roles of the PI3K/AKT/mTOR axis. *Curr Top Microbiol Immunol* **407**: 153–189. https://doi.org/10.1007/82_2017_6
- Arita K, Utsumi T, Kato A, Kanno T, Kobuchi H, Inoue B, Akiyama J, Utsumi K (2000) Mechanism of dibucaine-induced apoptosis in promyelocytic leukemia cells (HL-60). *Biochem Pharmacol* **60**: 905–915. [https://doi.org/10.1016/s0006-2952\(00\)00406-8](https://doi.org/10.1016/s0006-2952(00)00406-8)
- Cahill D, Turcan S (2018) Origin of gliomas. *Semin Neurol* **38**: 5–10. <https://doi.org/10.1055/s-0037-1620238>
- Cai J, Yi M, Tan Y, Li X, Li G, Zeng Z, Xiong W, Xiang B (2021) Natural product triptolide induces GSDME-mediated pyroptosis in head and neck cancer through suppressing mitochondrial hexokinase-IotaIota. *J Exp Clin Cancer Res* **40**: 190. <https://doi.org/10.1186/s13046-021-01995-7>
- Chan EW, Cheng SC, Sin FW, Xie Y (2001) Triptolide induced cytotoxic effects on human promyelocytic leukemia, T cell lymphoma and human hepatocellular carcinoma cell lines. *Toxicol Lett* **122**: 81–87. [https://doi.org/10.1016/s0378-4274\(01\)00353-8](https://doi.org/10.1016/s0378-4274(01)00353-8)
- Chen L, Wang J, Wu J, Zheng Q, Hu J (2018a) Indirubin suppresses ovarian cancer cell viabilities through the STAT3 signaling pathway. *Drug Des Devel Ther* **12**: 3335–3342. <https://doi.org/10.2147/DDDT.S174613>
- Chen SR, Dai Y, Zhao J, Lin L, Wang Y, Wang Y (2018b) A mechanistic overview of triptolide and celastrol, natural products from *Tripterygium wilfordii* Hook F. *Front Pharmacol* **9**: 104. <https://doi.org/10.3389/fphar.2018.00104>
- Chen XL, Geng YJ, Li F, Hu WY, Zhang RP (2022) Cytotoxic terpenoids from *Tripterygium hypoglaucom* against human pancreatic cancer cells SW1990 by increasing the expression of Bax protein. *J Ethnopharmacol* **289**: 115010. <https://doi.org/10.1016/j.jep.2022.115010>
- Christgen S, Zheng M, Kesavardhana S, Karki R, Malireddi RKS, Bantho B, Place DE, Briard B, Sharma BR, Tuladhar S, Samir P, Burton A, Kanneganti TD (2020) Identification of the PANoptosome: A molecular platform triggering pyroptosis, apoptosis, and necroptosis (PANoptosis). *Front Cell Infect Microbiol* **10**: 237. <https://doi.org/10.3389/fcimb.2020.00237>
- D'Arcy MS (2019) Cell death: a review of the major forms of apoptosis, necrosis and autophagy. *Cell Biol Int* **43**: 582–592. <https://doi.org/10.1002/cbin.11137>
- Fang T, Liu L, Liu W (2020) Network pharmacology-based strategy for predicting therapy targets of *Tripterygium wilfordii* on acute myeloid leukemia. *Medicine (Baltimore)* **99**: e23546. <https://doi.org/10.1097/MD.00000000000023546>
- Feng H, Cheng X, Kuang J, Chen L, Yuen S, Shi M, Liang J, Shen B, Jin Z, Yan J, Qiu W (2018) Apatinib-induced protective autophagy and apoptosis through the AKT-mTOR pathway in anaplastic thy-

- roid cancer. *Cell Death Dis* 9: 1030. <https://doi.org/10.1038/s41419-018-1054-3>
- Ferris SP, Hofmann JW, Solomon DA, Perry A (2017) Characterization of gliomas: from morphology to molecules. *Virchows Arch* 471: 257–269. <https://doi.org/10.1007/s00428-017-2181-4>
- Ghotme KA, Barreto GE, Echeverria V, Bustos RH, Sanchez M, Leszek J, Yarla NS, Gomez RM, Tarasov V, Ashraf GM, Aliev G (2017) Gliomas: New perspectives in diagnosis, treatment and prognosis. *Curr Top Med Chem* 17: 1438–1447. <https://doi.org/10.2174/1568026617666170103162639>
- Guo H, Golczer G, Wittner BS, Langenbacher A, Zachariah M, Dubash TD, Hong X, Comaills V, Burr R, Ebright RY, Horwitz E, Vuille JA, Hajizadeh S, Wiley DF, Reeves BA, Zhang JM, Niederhoffer KL, Lu C, Wesley B, Ho U, Nieman LT, Toner M, Vasudevan S, Zou L, Mostoslavsky R, Maheswaran S, Lawrence MS, Haber DA (2021) NR4A1 regulates expression of immediate early genes, suppressing replication stress in cancer. *Mol Cell* 81: 4041–4058 e15. <https://doi.org/10.1016/j.molcel.2021.09.016>
- Hanaei S, Afshari K, Hirbod-Mobarakeh A, Mohajer B, Amir Dastmalchi D, Rezaei N (2018) Therapeutic efficacy of specific immunotherapy for glioma: a systematic review and meta-analysis. *Rev Neurosci* 29: 443–461. <https://doi.org/10.1515/revneuro-2017-0057>
- Horibata S, Vo T V, Subramanian V, Thompson PR, Coonrod SA (2015) Utilization of the soft agar colony formation assay to identify inhibitors of tumorigenicity in breast cancer cells. *J Vis Exp* e52727. <https://doi.org/10.3791/52727>
- Hu M, Luo Q, Alitongbieke G, Chong S, Xu C, Xie L, Chen X, Zhang D, Zhou Y, Wang Z, Ye X, Cai L, Zhang F, Chen H, Jiang F, Fang H, Yang S, Liu J, Diaz-Meco MT, Su Y, Zhou H, Moscat J, Lin X, Zhang XK (2017) Celastrol-Induced Nur77 Interaction with TRAF2 alleviates inflammation by promoting mitochondrial ubiquitination and autophagy. *Mol Cell* 66: 141–153 e6. <https://doi.org/10.1016/j.molcel.2017.03.008>
- Kim MJ, Lee TH, Kim SH, Choi YJ, Heo J, Kim YH (2010) Triptolide inactivates Akt and induces caspase-dependent death in cervical cancer cells via the mitochondrial pathway. *Int J Oncol* 37: 1177–1185. https://doi.org/10.3892/ijo_00000769
- Lee KY, Chang W, Qiu D, Kao PN, Rosen GD (1999) PG490 (triptolide) cooperates with tumor necrosis factor-alpha to induce apoptosis in tumor cells. *J Biol Chem* 274: 13451–13455. <https://doi.org/10.1074/jbc.274.19.13451>
- Li J, Wu Y, Wang D, Zou L, Fu C, Zhang J, Leung GP (2019) Oridonin synergistically enhances the anti-tumor efficacy of doxorubicin against aggressive breast cancer via pro-apoptotic and anti-angiogenic effects. *Pharmacol Res* 146: 104313. <https://doi.org/10.1016/j.phrs.2019.104313>
- Li JX, Shi JF, Wu YH, Xu HT, Fu CM, Zhang JM (2021) Mechanisms and application of triptolide against breast cancer. *Zhongguo Zhong Yao Za Zhi* 46: 3249–3256 (in Chinese). <https://doi.org/10.19540/j.cnki.cjcm.20210225.601>
- Li X, Wu C, Chen N, Gu H, Yen A, Cao L, Wang E, Wang L (2016) PI3K/Akt/mTOR signaling pathway and targeted therapy for glioblastoma. *Oncotarget* 7: 33440–33450. <https://doi.org/10.18632/oncotarget.7961>
- Liu X, Zhao P, Wang X, Wang L, Zhu Y, Song Y, Gao W (2019) Celastrol mediates autophagy and apoptosis via the ROS/JNK and Akt/mTOR signaling pathways in glioma cells. *J Exp Clin Cancer Res* 38: 184. <https://doi.org/10.1186/s13046-019-1173-4>
- Lucia MB, Rutella S, Rumi C, Ventura G, Caldarola G, Cauda R (1997) Detection of P-glycoprotein efflux activity on peripheral blood lymphocyte subsets from HIV+ patients. *Eur J Histochem* 41 (Suppl 2): 195–196
- Luiz MT, Tofani LB, Araujo VHS, di Filippo LD, Duarte JL, Marchetti JM, Chorilli M (2021) Gene therapy based on lipid nanoparticles as non-viral vectors for glioma treatment. *Curr Gene Ther* 21: 452–463. <https://doi.org/10.2174/1566523220999201230205126>
- Meng HT, Zhu L, Ni WM, You LS, Jin J, Qian WB (2011) Triptolide inhibits the proliferation of cells from lymphocytic leukemic cell lines in association with downregulation of NF-kappaB activity and miR-16-1*. *Acta Pharmacol Sin* 32: 503–511. <https://doi.org/10.1038/aps.2010.237>
- Morshed RA, Young JS, Hervey-Jumper SL, Berger MS (2019) The management of low-grade gliomas in adults. *J Neurosurg Sci* 63: 450–457. <https://doi.org/10.23736/S0390-5616.19.04701-5>
- Nagata S (2018) Apoptosis and clearance of apoptotic cells. *Annu Rev Immunol* 36: 489–517. <https://doi.org/10.1146/annurev-immunol-042617-053010>
- Poff A, Koutnik AP, Egan KM, Sahebjam S, D'Agostino D, Kumar NB (2019) Targeting the Warburg effect for cancer treatment: Ketogenic diets for management of glioma. *Semin Cancer Biol* 56: 135–148. <https://doi.org/10.1016/j.semcancer.2017.12.011>
- Porta C, Paglino C, Mosca A (2014) Targeting PI3K/Akt/mTOR signaling in cancer. *Front Oncol* 4: 64. <https://doi.org/10.3389/fonc.2014.00064>
- Reifenberger G, Wirsching HG, Knobbe-Thomsen CB, Weller M (2017) Advances in the molecular genetics of gliomas – implications for classification and therapy. *Nat Rev Clin Oncol* 14: 434–452. <https://doi.org/10.1038/nrclinonc.2016.204>
- Sturm D, Pfister SM, Jones DTW (2017) Pediatric gliomas: current concepts on diagnosis, biology, and clinical management. *J Clin Oncol* 35: 2370–2377. <https://doi.org/10.1200/JCO.2017.73.0242>
- Wang J (2021) Tripterine and miR-184 show synergy to suppress breast cancer progression. *Biochem Biophys Res Commun* 561: 19–25. <https://doi.org/10.1016/j.bbrc.2021.04.108>
- Wei YS, Adachi I (1991) Inhibitory effect of triptolide on colony formation of breast and stomach cancer cell lines. *Zhongguo Yao Li Xue Bao* 12: 406–410
- Weng W, Goel A (2022) Curcumin and colorectal cancer: An update and current perspective on this natural medicine. *Semin Cancer Biol* 80: 73–86. <https://doi.org/10.1016/j.semcancer.2020.02.011>
- Xia P, Xu XY (2015) PI3K/Akt/mTOR signaling pathway in cancer stem cells: from basic research to clinical application. *Am J Cancer Res* 5: 1602–1609
- Xu S, Tang L, Li X, Fan F, Liu Z (2020) Immunotherapy for glioma: Current management and future application. *Cancer Lett* 476: 1–12. <https://doi.org/10.1016/j.canlet.2020.02.002>
- Xu W, Yang Z, Lu N (2015) A new role for the PI3K/Akt signaling pathway in the epithelial-mesenchymal transition. *Cell Adh Migr* 9: 317–324. <https://doi.org/10.1080/19336918.2015.1016686>
- Yang W, Guastella J, Huang JC, Wang Y, Zhang L, Xue D, Tran M, Woodward R, Kasibhatla S, Tseng B, Drewe J, Cai SX (2003) MX1013, a dipeptide caspase inhibitor with potent *in vivo* antiapoptotic activity. *Br J Pharmacol* 140: 402–412. <https://doi.org/10.1038/sj.bjp.0705450>
- Yang Y, Zhao M, Hu T, Su F, Qian F, Wang Z (2021) Identification of an antitumor effect of demethylzeylasteral on human gastric cancer cells. *Oncol Lett* 21: 49. <https://doi.org/10.3892/ol.2020.12310>
- You L, Dong X, Yin X, Yang C, Leng X, Wang W, Ni J (2018) Rhein induces cell death in HepaRG Cells through cell cycle arrest and apoptotic pathway. *Int J Mol Sci* 19: <https://doi.org/10.3390/ijms19041060>
- Zeng Y, Du WW, Wu Y, Yang Z, Awan FM, Li X, Yang W, Zhang C, Yang Q, Yee A, Chen Y, Yang F, Sun H, Huang R, Yee AJ, Li RK, Wu Z, Backx PH, Yang BB (2017) A circular RNA binds to and activates AKT phosphorylation and nuclear localization reducing apoptosis and enhancing cardiac repair. *Theranostics* 7: 3842–3855. <https://doi.org/10.7150/thno.19764>
- Zhang C, Sun PP, Guo HT, Liu Y, Li J, He XJ, Lu AP (2016) Safety profiles of *Tripterygium wilfordii* Hook F: A systematic review and meta-analysis. *Front Pharmacol* 7: 402. <https://doi.org/10.3389/fphar.2016.00402>
- Zhang LL, Zhang J, Shen L, Xu XM, Yu HG (2013) Overexpression of AKT decreases the chemosensitivity of gastric cancer cells to cisplatin *in vitro* and *in vivo*. *Mol Med Rep* 7: 1387–1390. <https://doi.org/10.3892/mmr.2013.1400>
- Zhou Y, Huang Y, Xu Q, Ye M, Sun C, Zhou D (2002) Several monomers from *Tripterygium wilfordii* inhibit proliferation of glioma cells in vitro. *Chin J Cancer* 21: 1106–1108
- Zhu Y, Liu X, Zhao P, Zhao H, Gao W, Wang L (2020) Celastrol suppresses glioma vasculogenic mimicry formation and angiogenesis by blocking the PI3K/Akt/mTOR signaling pathway. *Front Pharmacol* 11: 25. <https://doi.org/10.3389/fphar.2020.00025>